Supplementary information

Modification of Composite Catalytic Material $Cu_mV_nO_x$@CeO_2 Core-shell Nanorod by Tungsten for NH_3-SCR

Xiaosheng Huang[a,b], Fang Dong[a], Guodong Zhang[a] and Zhicheng Tang[a,c*]

(a. State Key Laboratory for Oxo Synthesis and Selective Oxidation, National Engineering Research Center for Fine Petrochemical Intermediates, Lanzhou Institute of Chemical Physics, Chinese Academy of Sciences, Lanzhou 730000, PR China

b. University of Chinese Academy of Sciences, Beijing 100039, PR China)

c. Dalian National Laboratory for Clean Energy, Dalian Institute of Chemical Physics, Chinese Academy of Sciences, Dalian, 116023, China

*Corresponding author. Tel.: +86-931-4968083, Fax: +86-931-8277088, E-mail address: tangzhicheng@licp.cas.cn (Z.Tang).

Fig. S1 TG/DTA curves of PVP (K90).

Fig. S2 TEM images of $Cu_mV_nO_x$ samples calcined at different temperatures.

Fig. S3 FTIR spectrum (a) and XRD patterns (b) of Ce-MOF, $Cu_mV_nO_x$-NF/Ce and $Cu_mV_nO_x$-NF@Ce-MOF.

Fig. S4 N_2 sorption curves and pore size distribution of all as-prepared catalysts.

Fig. S5 XPS spectra of $Cu_mV_nO_y$@CeO_2-WO_x calcined at different temperatures.

Table S1 Quantity results of surface acid sites.

Table S2 Peak integration area of pyridine FTIR and NH_3-TPD.

Table S3 XPS results of surface composition

Table S4. Reaction rate constant k of $Cu_3(VO_4)_2$, CeO_2, $Cu_3(VO_4)_2$@CeO_2 and $Cu_3(VO_4)_2$@CeO_2-WO_x.

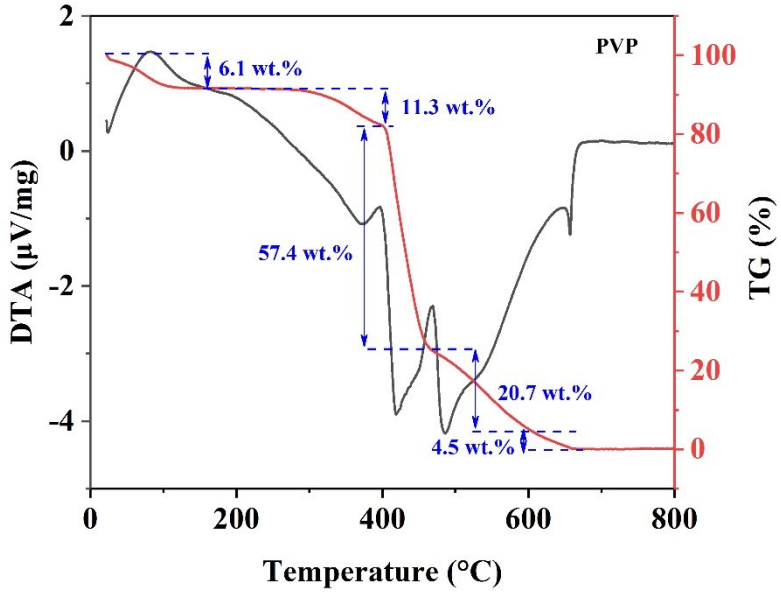

Fig. S1 TG/DTA curves of PVP (K90).

As shown in above TG/DTA curves, the decomposition of PVP (k90) mainly occurred in 290 ~ 410 °C with several exothermic peaks, which implied that the side and main chains were decomposed step by step. All residuum was completely consumed above 663 °C. Above information could provide references for other samples' TG/DTA analyses in text part.

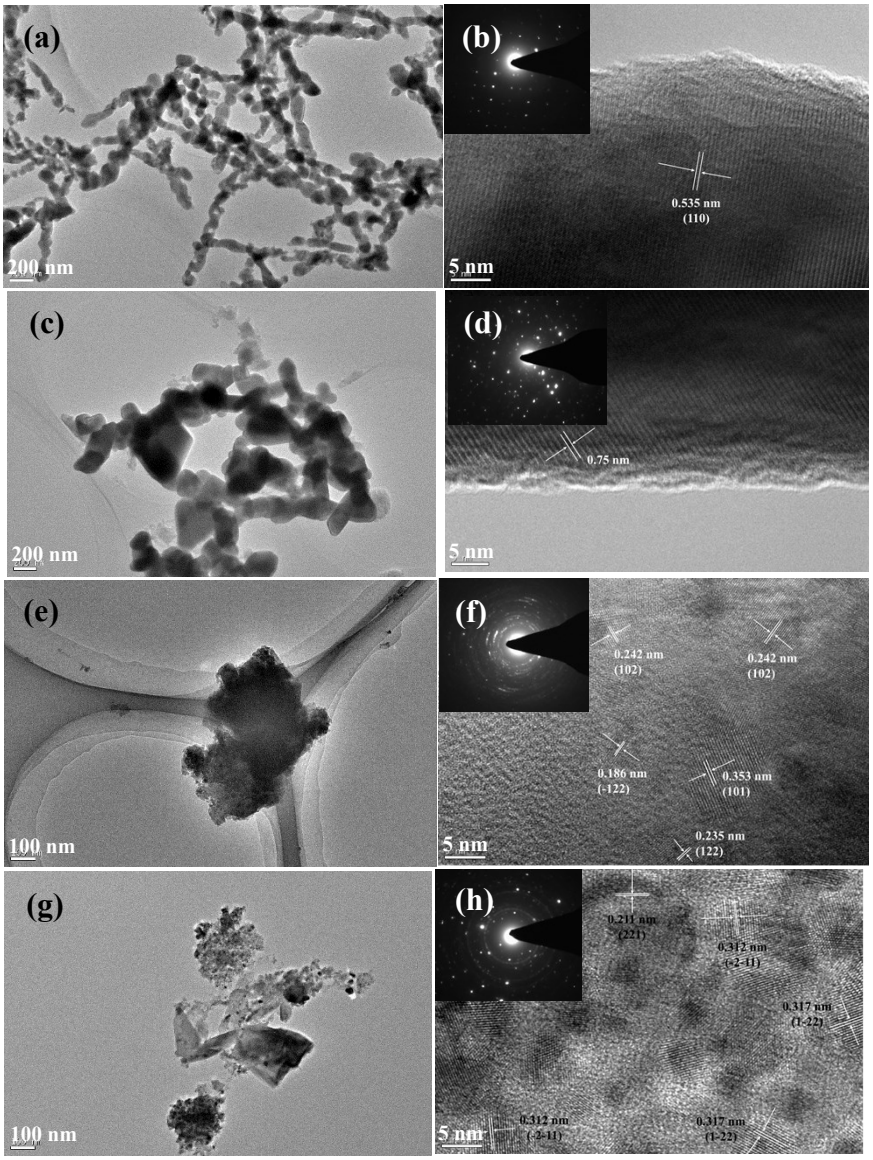

Fig. S2 TEM images of $Cu_mV_nO_x$ samples calcined at 400 °C (a, b), 500 °C (c, d), 600 °C (e, f) and 700 °C (g, h).

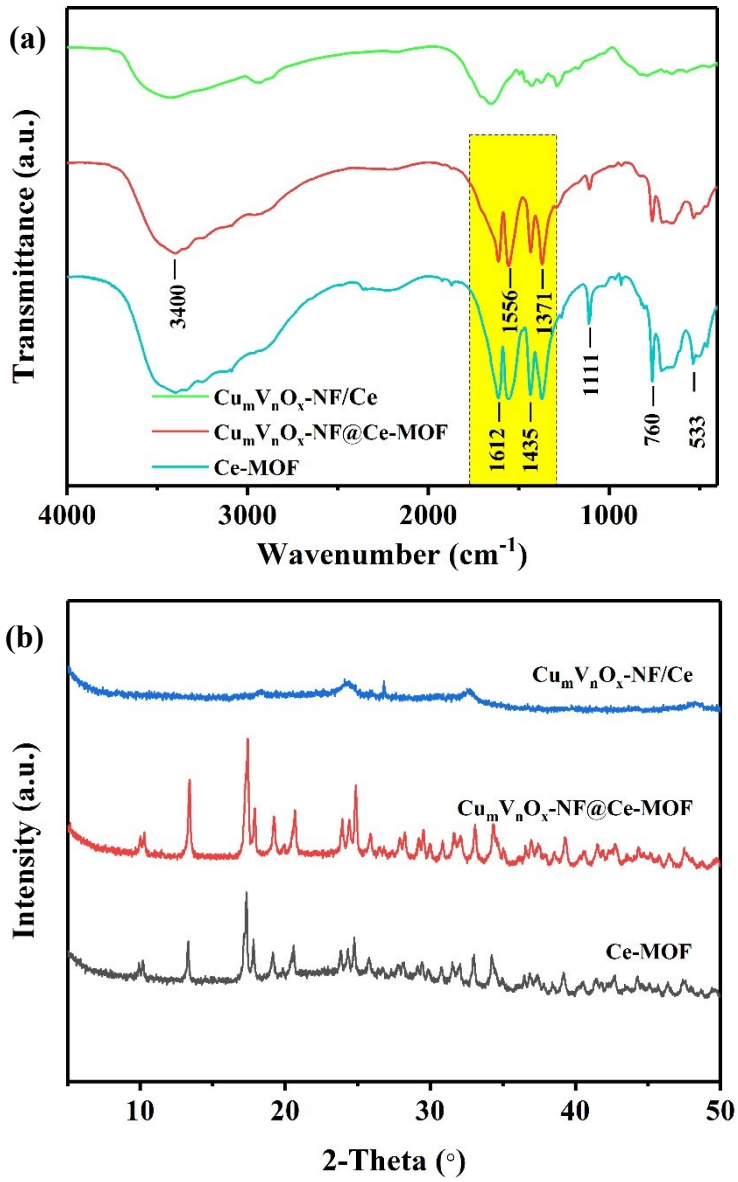

Fig. S3 FTIR spectrum (a) and XRD patterns (b) of Ce-MOF, $Cu_mV_nO_x$-NF@Ce-MOF and $Cu_mV_nO_x$-NF/Ce.

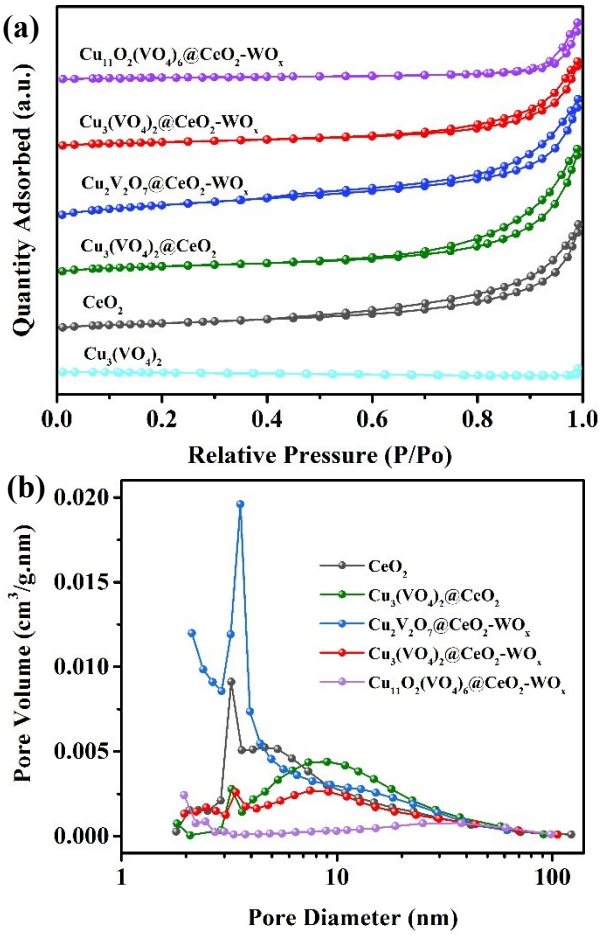

Fig. S4 N_2 sorption curves (a) and pore size distribution (b) of all as-prepared catalysts.

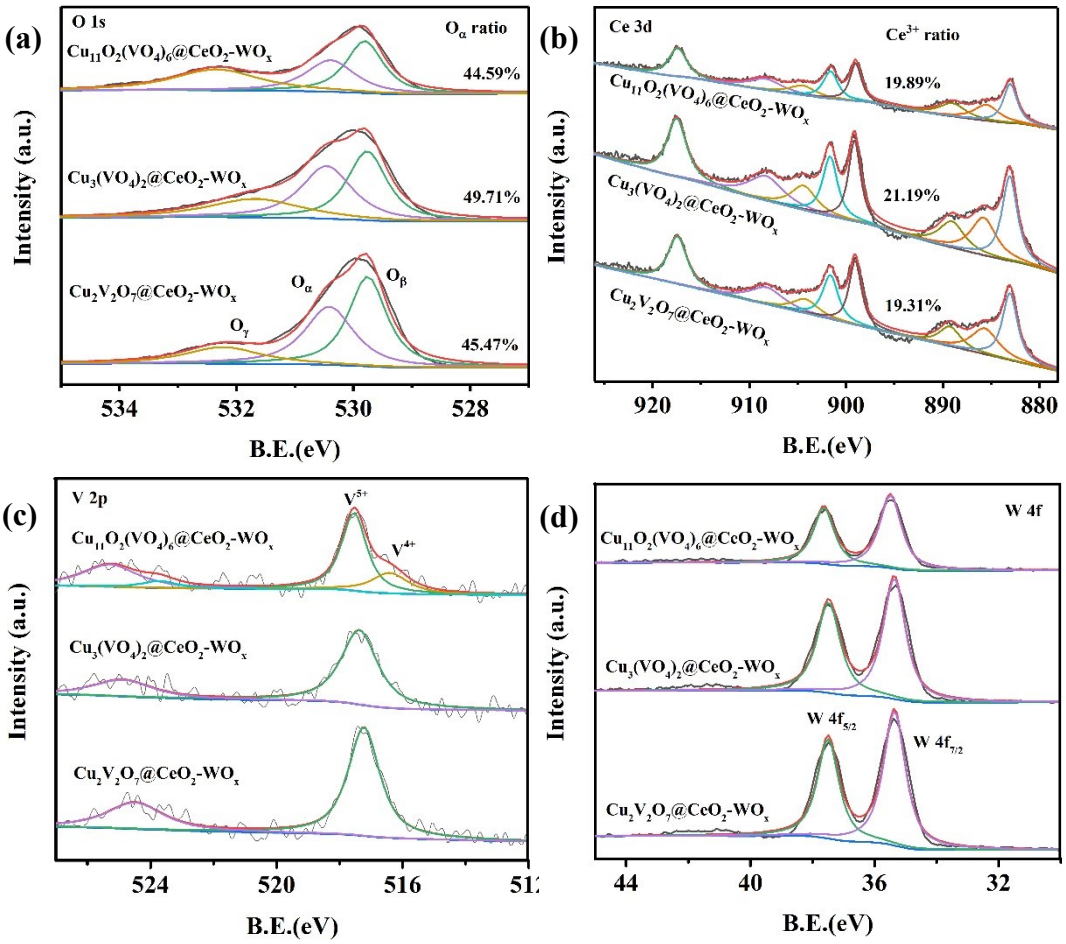

Fig. S5 XPS spectra of $Cu_mV_nO_y$@CeO_2-WO_x calcined at different temperatures.

Table S1 Quantity results of surface acid sites.

samples	NH_3 uptake (mmol/g_{cat})		
	Weak acid (<240 °C)	Medium strong acid (>240 °C)	total
$Cu_3(VO_4)_2$	-	1.15	1.15
CeO_2	0.48	-	0.48
$Cu_3(VO_4)_2@CeO_2$	-	1.04	1.04
$Cu_2V_2O_7@CeO_2$-WO_x	0.67	0.88	1.55
$Cu_3(VO_4)_2@CeO_2$-WO_x	1.30	1.29	2.59
$Cu_{11}O_2(VO_4)_6@CeO_2$-WO_x	0.65	0.24	0.89

Table S2 Peak integration area of pyridine FTIR and NH_3-TPD.

$Cu_3(VO_4)_2@CeO_2$-WO_x	Peak integration area (a.u.)		Area ratio
Pyridine FTIR	Lewis acid	Brønsted acid	0.96 [a]
	12.3	11.8	
NH_3-TPD	Weak acid	Medium strong acid	0.99 [b]
	145.2	144.8	

[a] the area ratio of Brønsted acid to Lewis acid

[b] the area ratio of Medium strong acid to Weak acid

Table S3 Catalysts surface composition (%)

	Cu	V	O	Ce	W	O_a ratio	Ce^{3+} ratio
$Cu_3(VO_4)_2$	12.42	28.99	58.59	-	-	49.12	-
$Cu_3(VO_4)_2$@ CeO_2	3.11	20.12	61.97	14.80	-	38.73	19.07
$Cu_2V_2O_7$@ CeO_2-WO_x	2.76	19.95	60.93	10.61	5.75	45.47	19.31
$Cu_3(VO_4)_2$@ CeO_2-WO_x	2.59	19.37	60.04	12.86	5.14	49.71	21.19
$Cu_{11}O_2(VO_4)_6$@ CeO_2-WO_x	2.61	20.66	63.15	8.76	4.81	44.59	19.89

Table S4. Reaction rate constant k of $Cu_3(VO_4)_2$, CeO_2, $Cu_3(VO_4)_2$@CeO_2 and $Cu_3(VO_4)_2$@CeO_2-WO_x.

Temperature (°C)	Reaction rate constant k ($L \cdot g^{-1} \cdot min^{-1}$)			
	$Cu_3(VO_4)_2$	CeO_2	$Cu_3(VO_4)_2$@CeO_2	$Cu_3(VO_4)_2$@CeO_2-WO_x
100	0.02	0.02	0.03	0.09
140	0.04	0.03	0.10	0.39
180	0.07	0.06	0.22	1.02
220	0.10	0.14	0.42	1.61